J Mater Sci (2009) 44:3223–3228
DOI 10.1007/s10853-009-3430-y

Microstructures and properties of $Bi_{3.25}La_{0.75}Ti_{2.94}V_{0.06}O_{12}$ ferroelectric thin film deposited by sol–gel method

Jianjun Li · Jun Yu · Jia Li · Bin Zhou · Guangxing Zhou · Yubin Li · Junxiong Gao · Yunbo Wang

Received: 26 October 2008 / Accepted: 20 March 2009 / Published online: 7 April 2009

Abstract $Bi_{3.25}La_{0.75}Ti_{2.94}V_{0.06}O_{12}$ (BLTV) thin film was fabricated on the $Pt/TiO_2/SiO_2/p\text{-}Si(100)$ substrate using sol–gel method. The microstructures and electrical properties of the film after cosubstitution of La and V were investigated. The BLTV thin film shows less highly *c*-axis oriented than the BIT thin film mainly with fine rod-like grains. Raman spectroscopy shows that TiO_6 (or VO_6) symmetry decreases and Ti–O (or V–O) hybridization increases for V substitution. The P_r and E_c values of the BLTV thin film are 26.3 μC/cm^2 and 98 kV/cm at a voltage of 12 V, respectively. The thin film also exhibits a very strong fatigue endurance up to 10^{10} cycles and low leakage current density. The excellent properties of the BLTV thin film are attributed to the effective decrease or suppression of oxygen vacancies after La and V cosubstitution in the thin film.

Introduction

Ferroelectric materials have been extensively studied for applications in nonvolatile random access memories (NvRAM) [1, 2]. Bismuth titanate [$Bi_4Ti_3O_{12}$ (BIT)] films have been recognized as the promising film materials due to their excellent fatigue-free nature, lead-free chemical composition, and other good electric properties. The BIT is monoclinic with the space group B1a1 and with the lattice constant of the *c*-axis ($c = 3.2843$ nm). This value is considerably larger than that of the other two axis ($a = 0.5445$ nm, $b = 0.5411$ nm) at room temperature. The BIT has a spontaneous polarization in the *a*–*c* plane and exhibits two independently reversible components along the *c* and *a* axes [3, 4]. It shows spontaneous polarization values of 4 and 50 μC/cm^2 along the *c* and *a* axes, respectively. The ferroelectric properties of these bismuth layer-structured thin films are mostly influenced by the orientation of the films [5]. For BIT thin films, because the BIT thin films are highly *c*-axis oriented, the spontaneous polarization is much lower than that for *a*-axis oriented [6]. Recently, it was reported that some A-site or B-site substituted BIT showed large remanent polarizations (P_r). In the case of A-site substitution in BIT, La-substituted BIT [$Bi_{3.25}La_{0.75}Ti_3O_{12}$ (BLT)] films exhibited enhanced P_r of 12 μC/cm^2 with high fatigue resistance, which make them applicable to direct commercialization [7, 8]. Other lanthanides, such as Nd, Pr, Sm, etc., result in similar results [9–11]. In the case of B-site substitution in BIT, some donor ions, such as V^{5+}, Nd^{5+}, W^{6+}, could effectively decrease the space charge density resulting in the improvement of the ferroelectric properties [12–14]. For further improvement of the ferroelectric properties, A and B sites cosubstitution by various ions should be considered because the properties of BIT-based materials strongly depend on species of the substituent ions. In this paper, La and V-cosubstituted BIT [$Bi_{3.25}La_{0.75}Ti_{2.94}V_{0.06}O_{12}$ (BLTV)] thin film was fabricated on the $Pt/TiO_2/SiO_2/p\text{-}Si(100)$ substrate using sol–gel method. The effect of cosubstitution of La and V on structural and electrical properties of the BIT thin film was investigated.

J. Li (✉) · J. Yu · J. Li · B. Zhou · G. Zhou · Y. Li · J. Gao · Y. Wang
Department of Electronic Science and Technology, Huazhong University of Science and Technology, 430074 Wuhan, People's Republic of China
e-mail: jjlhust@yahoo.com.cn

Experimental

The BLTV thin film was prepared on $Pt/TiO_2/SiO_2$/p-Si(100) substrate by sol–gel processes. The precursor solution for BLTV film was prepared from Bismuth nitrate [$Bi(NO_3)_3 \cdot 5H_2O$], lanthanum nitrate [$La(NO_3)_3 \cdot xH_2O$], titanium butoxide [$Ti(OC_4H_9)_4$], and vanadium oxytripropoxide [$VO(C_3H_7O)_3$]. The bismuth nitrate and lanthanum nitrate were dissolved in 2-methoxyethanol, while titanium butoxide and vanadium oxytripropoxide were stabilized by acetylacetone. The BLTV precursor was obtained by mixing these two solutions with a molar concentration of 0.1 mol/L. A 10 mol.% excess amount of bismuth nitrate was used to compensate Bi evaporation during the heat treatment. The BLTV precursor solution was spin-coated on $Pt/TiO_2/SiO_2$/p-Si(100) substrate at 3,700 rpm for 30 s. Then, the sol film was dried at 300 °C for 5 min and pyrolyzed at 400 °C for 10 min to remove residual organic compounds. These processes were repeated six times to achieve the desired film thickness (~380 nm). Then the film was annealed at 750 °C for 30 min under air ambient in a horizontal quartz-tube furnace. After these processes, Pt top electrodes with an area of about 7×10^{-4} cm^2 were deposited by means of sputtering using a shadow mask for electrical measurements. Furthermore, the unsubstituted BIT thin film was also fabricated by the same method for the comparison with the BLTV thin film.

The phase identification, crystalline orientation, and degree of crystallinity of the prepared film was studied by a χ' Pert PRO X-ray diffractometer (PANalytical B. V. Co., the Netherlands) with Cu-Ka radiation at 40 kV. The local microstructure and local symmetry of the film were also characterized by Raman spectroscopy (LabRam HR800, Horiba Jobin Yvon Co., France). The Raman measurements were performed at room temperature using the 514.5 nm line of an argon ion laser as the excitation source. The surface morphologies were investigated using Sirion a 200 field-emission scanning electron microscope (FEI Co., the Netherlands). The *P–E* hysteresis loops and fatigue were measured by using a RT66A ferroelectric test system (Radiant Technology Inc., USA), and the leakage current was measured by a Keithley 2400 source meter (Keithley Instruments Inc., USA), and the current–voltage data were measured using a staircase mode with the appropriate hold time.

Results and discussion

Figure 1 shows the X-ray diffraction spectroscopy (XRD) patterns of the BLTV and BIT thin films. All the diffraction peaks can be indexed according to the reference pattern of

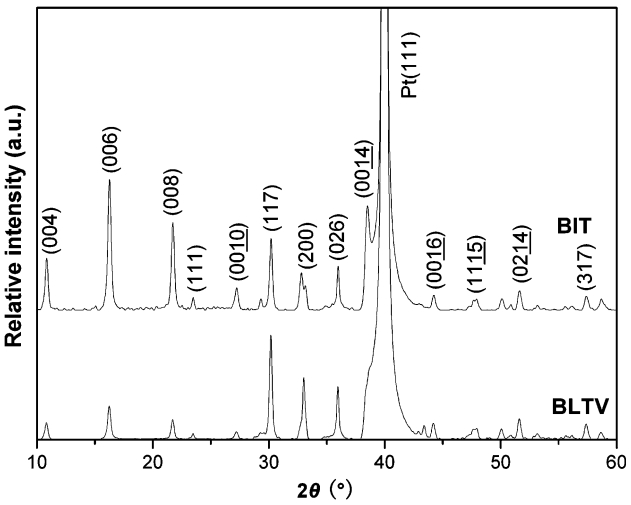

Fig. 1 XRD patterns of the BLTV and BIT thin films deposited on the $Pt/TiO_2/SiO_2$/p-Si(100) substrates

$Bi_4Ti_3O_{12}$ powder [BIT, JCPDS (Joint Committee on Powder Diffraction Standards) 35-795]. The good agreement in XRD peaks of BLTV film with those of BIT indicates that the lattice structure of the BLTV is similar to that of BIT. The X-ray diffraction pattern shows the BLTV thin film is single layer-structured perovskite phase and no pyrochlore phase. To investigate the effect of substitution on the structure of the BIT thin film, the *c*-axis orientation degree for the BIT and BLTV thin films is described by the diffraction intensity ration of the (00*l*) peaks to all the peaks [15, 16],

$$f(00l) = \frac{\sum I(00l)}{\sum I(hkl)} \quad (1)$$

where $I(00l)$ and $I(hkl)$ are the peak intensities for *c*-axis and (hkl) diffractions, respectively. The *f* values obtained for the BIT and BLTV thin films corresponding to Fig. 1 are 72.9% and 26.2%, respectively. The relative intensity ratio of *c*-axis orientation for the BIT thin film is larger than that for the BLTV thin film. Thus, the BLTV thin film exhibits much less highly *c*-axis oriented, compared with the BIT thin film. And substitution increases the degree of non-*c*-axis orientation for the BIT thin film.

The typical unsubstituted BIT films have a strong tabular habit with the *c*-axis orientation, for the energy of the $\{00l\}$ surfaces, which is lower, and consequently the $\{h00\}$ and $\{0k0\}$ faces grow more rapidly. For La-substituted BIT thin films ($Bi_{4-x}La_xTi_3O_{12}$), controlling La substitution *x* to a certain extent can decrease *c*-axis orientation degree [17]. For B-site substituted BIT thin films, the degree of *c*-axis orientation decreases greatly with different donor ions substitution [18]. The substitution may break down the Ti–O chains due to the differences in the electron affinities, which results in the clusters in the precursor favoring the

growth of non-*c*-axis orientation. Thus, the cosubstituted BLTV thin film exhibits less highly *c*-axis oriented than the typical unsubstituted BIT thin film, and substitution can influence the orientation of the BIT thin film greatly.

The Raman spectra for the BLTV thin film sample was investigated in the Raman frequency shift range of 100–1,000 cm^{-1} as presented in Fig. 2 with BIT spetra. For bismuth layer-structured ferroelectrics (BLSFs), their phonon modes can generally be classified into two categories: low frequency modes below 200 cm^{-1} and high frequency modes above 200 cm^{-1} [19]. The low frequency modes below 200 cm^{-1} are related to large atomic masses, which reflect the vibration of Bi^{3+} ions in $(Bi_2O_2)^{2+}$ layer and A-site Bi^{3+} ions. The high frequency modes above 200 cm^{-1} reflect the vibration of Ti^{4+} and TiO_6 octahedron.

The phonon modes at 118 and 147 cm^{-1} reflect the vibration of A-site Bi^{3+} ions in layer-structured perovskite, and these modes shift to higher frequencies after cosubstitution in the BIT thin film. The average masses of La/Bi decrease, for La atomic mass is lower than Bi atomic mass ($M_{La}/M_{Bi} = 139/208$), so the related modes show upshift, which also indicates A-site Bi^{3+} ions in BIT film are partly substituted for La^{3+}. The 231 and 270 cm^{-1} modes are considered to reflect the distortion modes of TiO_6 octahedron. The 231 cm^{-1} mode is Raman inactive when the symmetry of the TiO_6 octahedron is O_h, but it becomes Raman active when distortion occurs in TiO_6 octahedron. The 565 cm^{-1} mode is attributed to a combination of stretching and bending of TiO_6 octahedron, while the 852 cm^{-1} mode is a pure stretching of TiO_6 octahedron. The disappearance of the 231 cm^{-1} mode and downshift of 270 cm^{-1} mode for the BLTV thin film could be explained by a decrease in distortion of TiO_6 due to the substitution of V for Ti, because V ions (V^{5+}, 0.0580 nm) have a little smaller size compared with Ti ions (Ti^{4+}, 0.0605 nm) [20, 21]. The smaller mass difference ($M_{Ti}/M_V = 47/50$) between Ti and V is not sufficient to lead to the observed changes in the Raman spectra at higher frequency, but that the observed changes are consistent with a change in the distortion of the $(Ti,V)O_6$ octahedron. Thus, the shift in the higher frequency could be attributed to the size difference between Ti and V ions.

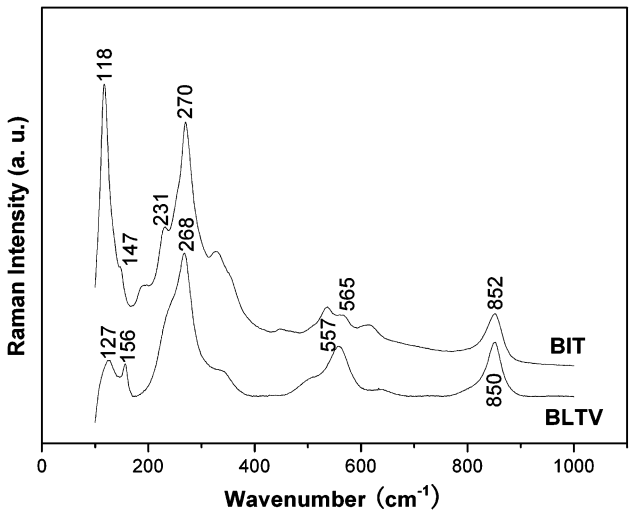

Fig. 2 Raman spectra of the BLTV and BIT thin films

The downshift of 565 and 852 cm^{-1} modes implies a little decrease in O_h symmetry of TiO_6 octahedron. For V-substituted BIT ($Bi_4Ti_{2.94}V_{0.06}O_{12}$), the 852 cm^{-1} mode exhibits downshift [22]. Since V is electronically more active than Ti, and there is a little asymmetry of TiO_6, an increase in Ti–O hybridization is implied. For La-substituted BIT ($Bi_{4-x}La_xTi_3O_{12}$), the 565 cm^{-1} mode shows the change in upshift with La content x increasing, while the 852 cm^{-1} mode remains unchanged [17]. Since La has no outer electrons and bonds slightly differently in the same lattice than lone-pair cations such as Bi or Pb, it exhibits less electronically active than Bi and less hybridization with the O 2*p* orbital, which strengthens the short-range repulsion and leads to decrease in distortion and increase in symmetry for TiO_6. Thus, the changes in the high-frequency portion of the Raman spectra are partly the result of La substitution altering the octahedral symmetry and distortion in addition to the effect of the B-site substitution.

Figure 3 shows the field-emission scanning electron microscopy (FE-SEM) surface morphologies of the BLTV and BIT thin films. A dense microstructure without any crack is obtained, as shown in Fig. 3. It can be seen that the BIT thin film is mainly composed of fine plate-like grains, while the BLTV film is mainly composed of fine rod-like grains. For BIT based films, the plate-like grains are related to the growth of *c*-axis orientation. Thus, the BLTV thin film is less highly *c*-axis oriented than the BIT thin film, which is consistent with the result of the XRD patterns above [23].

Figure 4a shows the polarization–voltage (*P*–*V*) curves of the BLTV thin film capacitor at various applied voltage with a cycle frequency of 7.5 kHz. As presented in this figure, the remanent polarization (P_r) and the coercive voltage increase with increasing applied voltage in the studied voltage range. The saturation properties of the P_r and E_c (the coercive field) values of the BLTV thin film are shown in Fig. 4b. When the applied voltage is smaller, the P_r and E_c increase rapidly with the increasing electric field. Whereas when the applied voltage is up to a certain value, the P_r and E_c increase slowly with the increasing voltage, approaching to a saturation status. The BLTV capacitor is characterized by a well-saturated *P*–*V* curve at an applied voltage of 12 V, giving the P_r and E_c values of 26.3 μC/cm^2 and 98 kV/cm, respectively. The *P*–*V* curves of the BLTV

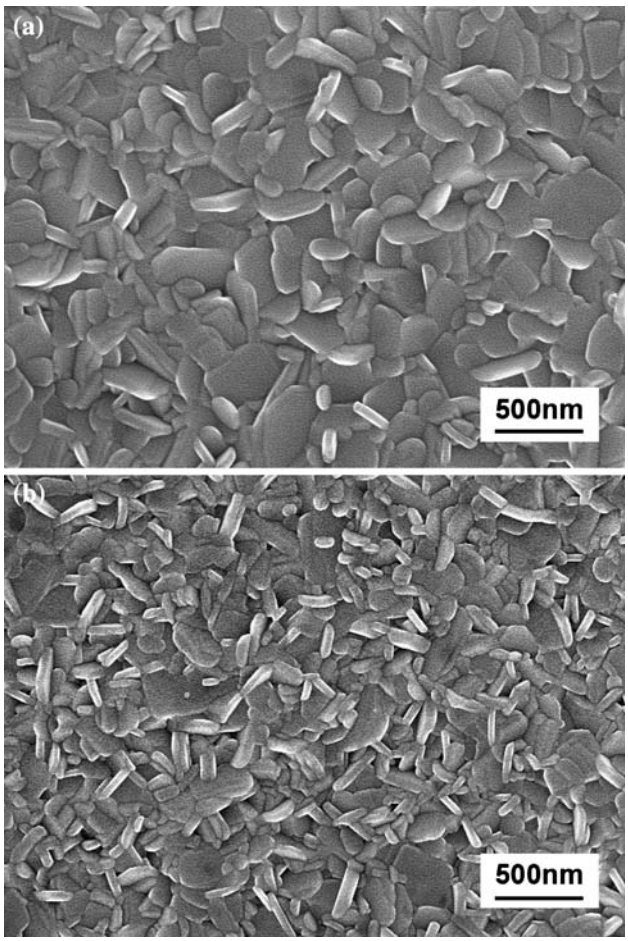

Fig. 3 FE-SEM surface morphologies of the **a** BIT and **b** BLTV thin films

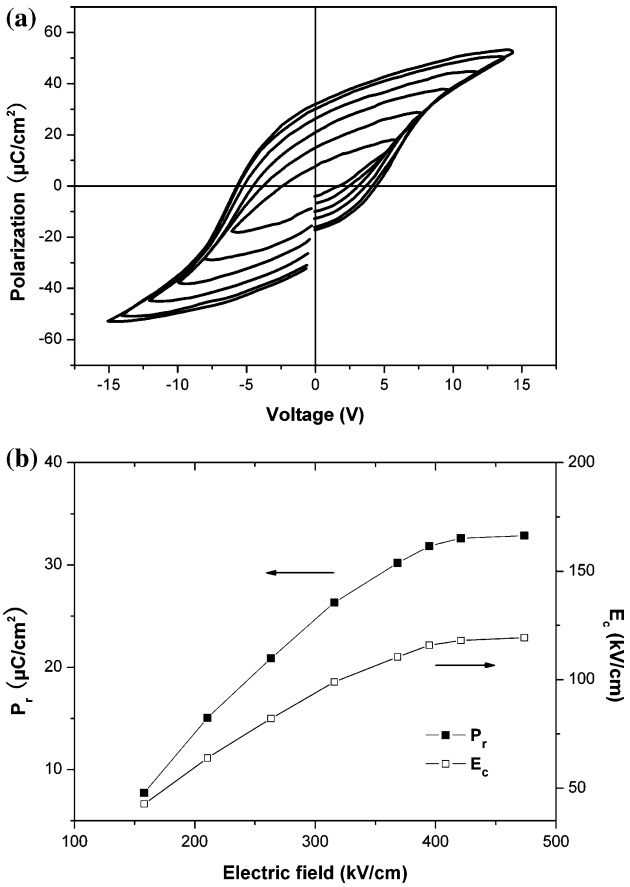

Fig. 4 **a** Polarization–voltage (*P*–*V*) hystersis loops of the BLTV thin film at various applied voltage. **b** P_r and E_c of the BLTV thin film as a function of applied electric field

and BIT thin film capacitors at the voltage of 12 V are shown in Fig. 5. The much larger P_r of the BLTV thin film compared with the BIT thin film could be explained by the increase of the degree of non-*c*-axis orientation, and the increase of Ti(V)–O hybridization inside $(Ti,V)O_6$, for there is less contribution of La to the Ti–O hybridization. As hybridization is essential to ferroelectricity, the increase of hybridization may increase the polarization [24].

Figure 6 illustrates the fatigue characteristics of the BLTV and BIT thin films. The test was performed at room temperature using 12 V, 100 kHz bipolar square pulses. From the figure we can see that, as the switching cycles increase, the normalized P_r (the P_r to the initial polarization) of the BLTV thin film decreases silghtly, while that of the BIT thin film decreases greatly. The fatigue test exhibits a very strong fatigue endurance up to 10^{10} cycles for the BLTV thin film.

Figure 7 shows the leakage current density of the BLTV and BIT thin film versus the applied electric field. The magnitude of dc leakage current is usually one of the most concerned factors for FeRAM application of ferroelectric thin films, due to its direct relation to power consumption and function failure of devices [25]. The leakage current density of the BLTV thin film is smaller than that of the BIT thin film. For the BLTV thin film, the leakage current

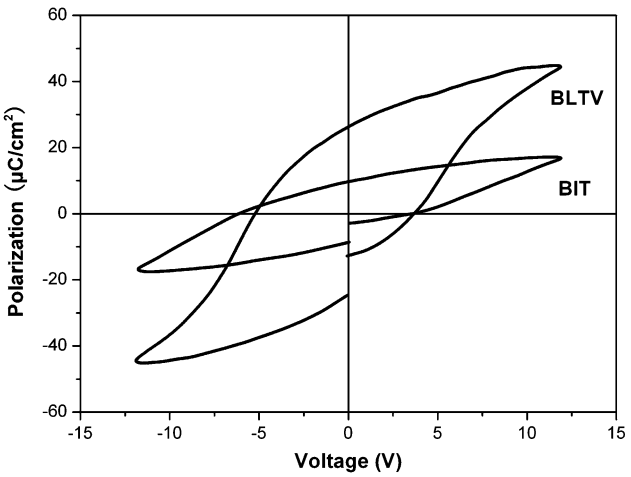

Fig. 5 Polarization–voltage (*P*–*V*) hystersis loops of the BLTV and BIT thin films at the voltage of 12 V

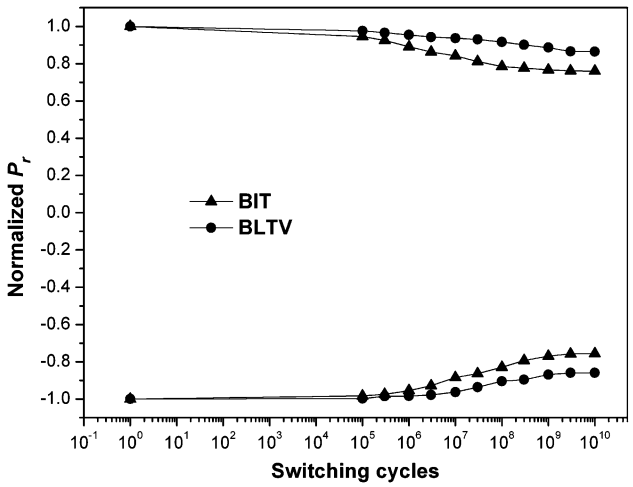

Fig. 6 Fatigue characteristics of the BLTV and BIT thin films with repetitive switching cycles

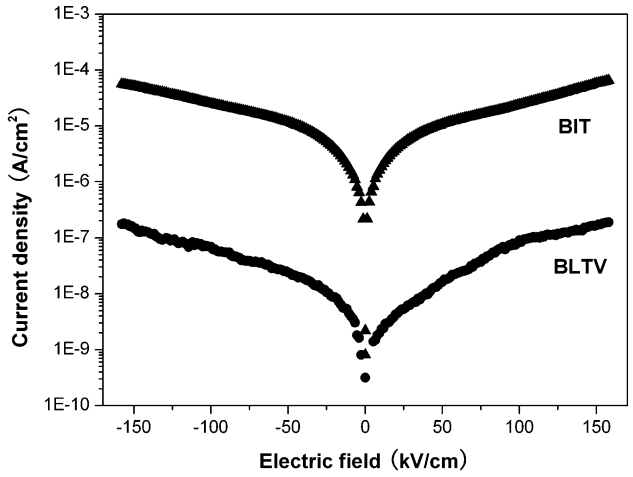

Fig. 7 Electric field dependence of leakage current density for the BLTV and BIT thin films

density increases gradually at low electric field, but generally in the order of 10^{-9}–10^{-8} A/cm^2 below 100 kv/cm. And the leakage current density is about 9×10^{-8} A/cm^2 at 100 kv/cm.

The excellent ferroelectric property, fatigue endurance and leakage current characteristic after La and V cosubstitution are attributed to the decrease of the defects, such as oxygen vacancies. For BLSF materials, the oxygen ions near the Bi ions are not stable, and some oxygen vacancies $\left(V_{\mathrm{o}}^{\cdot\cdot}\right)$ and Bi vacancies $\left(V_{\mathrm{Bi}}^{\prime\prime\prime}\right)$ are generated unavoidably due to the volatilization of Bi during the annealing processes under high temperatures [26]. This correlation can be expressed as follows:

$$\mathrm{Bi}^{3+} + xe^{-} \leftrightarrow \mathrm{Bi}^{+3-x} \tag{2}$$

$$\mathrm{O_O} \leftrightarrow \frac{1}{2}\mathrm{O_2} + V_{\mathrm{o}}^{\cdot\cdot} + 2e \tag{3}$$

It indicates that the formation of oxygen vacancies in layer-structured perovskite phase are related to the fragility of Bi–O bonds rather than the volatilization of Bi. Thus, Bi and oxygen vacancies can be reduced greatly by substituting La for Bi, not by simply using additional Bi excess, for La is more stable in layer-structured perovskite structure.

The oxygen vacancies are the hole trappers and act as the space charge. And they cause strong domain pinning with repetitive switching cycles, which deteriorates the properties of the ferroelectric films [27]. Better chemical stability of the perovskite layers against oxygen vacancies after substitution of some A-site Bi atoms for La atoms is helpful to the fatigue behavior and leakage current characteristic [28]. Furthermore, the substitution of the B-site Ti^{4+} for the donor-type V^{5+} can suppress the generation of oxygen vacancies due to the charge neutrality restriction [29]:

$$\mathrm{V_2O_5} \leftrightarrow 2V_{\mathrm{Ti}}^{\cdot} + 5\mathrm{O_O} + 2e \tag{4}$$

$$\frac{1}{2}\mathrm{O_2} + V_{\mathrm{o}}^{\cdot\cdot} + 2e \leftrightarrow \mathrm{O_O} \tag{5}$$

$$\mathrm{Bi} + V_{\mathrm{Bi}}^{\prime\prime\prime} + 3V_{\mathrm{Ti}}^{\cdot} \leftrightarrow \mathrm{Bi_{Bi}} + 3V_{\mathrm{Ti}} \tag{6}$$

where $V_{\mathrm{Ti}}^{\cdot}$ is the V ion with +1 effective charge at the Ti site, V_{Ti} is the V at the Ti, $\mathrm{O_O}$ is oxide in the lattice, $\mathrm{Bi_{Bi}}$ is Bi in the lattice, and e is the compensatory charge. Thus, $V_{\mathrm{Bi}}^{\prime\prime\prime}$, the tervalent negative electric center, is neutralized by $V_{\mathrm{Ti}}^{\cdot}$, and the oxygen vacancies are suppressed by the higher valentcation substitution. So the cosubstitution of A-site La and B-site V in the BIT thin film can improve the properties of the ferroelectric thin film effectively.

Conclusion

The BLTV thin film was fabricated on the Pt/$\mathrm{TiO_2}$/$\mathrm{SiO_2}$/p-Si(100) substrate using sol–gel method. The microstructures and electrical properties of the film after cosubstitution of La and V were investigated. The BLTV thin film shows less highly c-axis oriented than the BIT thin film mainly with fine rod-like grains revealed from the FE-SEM surface morphology. Raman spectroscopy shows $\mathrm{TiO_6}$ (or $\mathrm{VO_6}$) symmetry decreases and Ti–O (or V–O) hybridization increases for V substitution. The BLTV film capacitor is characterized by a well-saturated P–V curve at an applied voltage of 12 V, giving the P_{r} and E_{c} values of 26.3 μC/cm^2 and 98 kV/cm, respectively. The fatigue test exhibits a very strong fatigue endurance up to 10^{10} cycles. The leakage current density is generally in the order of

10^{-9}–10^{-8} A/cm^2 below 100 kv/cm. The excellent properties of the BLTV thin film are attributed to the effective decrease or suppression of oxygen vacancies after La and V cosubstitution in the thin film.

Acknowledgements This work is supported by the Key program of National Nature Science Foundation of China, Nos. 90407023 and 60571009. The authors gratefully acknowledge technical assistance from Analytical and Testing Center of Huazhong University of Science and Technology, China.

References

1. Scott JF, Araujo CA (1989) Science 246:1400
2. Haertling GH (1999) J Am Ceram Soc 82:797
3. Takenaka T, Sanaka K (1980) Jpn J Appl Phys 19:31
4. Ramesh R, Luther K, Wilkens B, Hart DL, Wang E, Trascon JM (1990) Appl Phys Lett 57:1505
5. Simoes AZ, Pianno RFC, Ries A, Varela JA, Longo E (2006) J Appl Phys 100:084106
6. Fuierer P, Li B (2002) J Am Ceram Soc 85:299
7. Park BH, Kang BS, Bu SD, Noh TW, Lee J, Jo W (1999) Nature 401:682
8. Chon U, Jang HM, Kim MG, Chang CH (2002) Phys Rev Lett 89:087601
9. Watanabe T, Funakubo H, Osada M, Uchida H, Okada I (2005) J Appl Phys 98:024110
10. Chon U, Shim JS, Jang HM (2003) J Appl Phys 93:4769
11. Chen M, Liu ZL, Wang Y, Wang CC, Yang XS, Yao KL (2004) Phys B 352:61
12. Kim SS, Song TK, Kim JK, Kim J (2002) J Appl Phys 92:2213
13. Kim JK, Kim J, Song TK, Kim SS (2002) Thin Solid Films 419:225
14. Lin WT, Chiu TW, Yu HH, Lin JL, Lin MS (2003) J Vac Sci Technol A 21:787
15. Lotgering FK (1959) J Inorg Nucl Chem 9:113
16. Lu CJ, Qiao Y, Qi YJ, Chen XQ, ZHU JS (2005) Appl Phys Lett 87:222901
17. Yau CY, Palan R, Tran K, Buchanan RC (2005) Appl Phys Lett 86:032907
18. Choi EK, Kim SS, Kim JK, Bae JC, Kim WJ, Lee YI, Song TK (2004) Jpn J Appl Phys 43:237
19. Shulman HS, Damjanovic D, Setter N (2000) J Am Ceram Soc 83:528
20. Li W, Yin Y, Su D, Zhu JS (2005) J Appl Phys 97:084102
21. Chen SY, Lan BC, Taso CS (2002) J Appl Phys 91:10032
22. Mao XY, He JH, Zhu J, Chen XB (2006) J Appl Phys 100:044104
23. Li J, Yu J, Peng G, Wang YB, Zhou WL (2007) J Phys D Appl Phys 40:3788
24. Cohen RE (1992) Nature 358:136
25. Araujo CA, Mcmillan LD, Melnick BM, Cuchiaro JD, Scott JF (1990) Ferroelectrics 104:241
26. Chu MW, Ganne M, Caldes MT, Gautier E, Brohan L (2003) Phys Rev B 68:014102
27. Park CH, Chadi DJ (1998) Phys Rev B 57:R13961
28. Kang BS, Park BH, Bu SD, Kang SH, Noh TW (1999) Appl Phys Lett 75:2644
29. Sun H, Zhu J, Fang H, Chen XB (2006) J Appl Phys 100:074102